Binaural Adaptive Feedback Cancellation Based on Prediction Error Method Using Interaural Level Differences in Hearing Device

Yuto Ueda* Hidetoshi Nakashima* Yuuki Yuno† and Nobuhiko Hiruma†
* National Institute of Technology, Kumamoto College, Kumamoto, Japan
E-mail: ae21ueda@g.kumamoto-nct.ac.jp, nakashi@kumamoto-nct.ac.jp
† Rion Co., Ltd., Tokyo, Japan
E-mail: y-yuno@rion.co.jp, n-hiruma@rion.co.jp

***Abstract*—In a system such as a hearing aid or hearing assistance device, a closed-loop may cause an oscillation phenomenon that limits the usability of the device. Feedback estimation using the least-mean-square-based algorithm is commonly used in devices with limited computing capacity; in this method, estimation errors occur when the input signals are highly autocorrelated, resulting in the generation of an acoustic artifact called entrainment. To solve this problem, decorrelation using a linear prediction error filter has been proposed. However, when the prediction error filter converges before howling is suppressed, the howling signal is also decorrelated, which may make it difficult to control howling.**

In this paper, we propose a binaural feedback canceller based on the prediction error method. The proposed method can solve both the howling and entrainment problems by using the interaural level difference to determine whether the input signals include howling signals or not. The results of computer simulation demonstrate the effectiveness of the proposed method improved sound quality and feedback estimation.

I. Introduction

Oscillation due to acoustic feedback is caused by the occurrence of a closed-loop when a loudspeaker and a microphone are in the same space, for example, in public address and sound reinforcement systems. Similarly, a closed-loop can occur in hearing aids and other hearing devices such as personal sound amplification products. Because these devices must be miniaturized, the distance between loudspeakers (known as receiver in hearing aid) and microphones is short. Therefore, a closed-loop can occur owing to the feedback of part of the output signal. Additionally, these devices amplify an input signal to compensate for hearing loss; the degree of amplification processing depends on the level of hearing loss. The repeated amplification of the feedback signal results in a type of oscillation called howling, which can discourage users from using hearing devices.

Many approaches to modeling and canceling acoustic feedback have been suggested[1], [2]. The least-mean-square (LMS) based algorithm is widely used in devices with limited computational capacity. Estimation bias occurs when the LMS based algorithm estimates the external feedback path using an input signal with high autocorrelation[3], [4]. The estimation error resulting from bias causes problematic distortion of the input signal and produces an artifact called entrainment[5]. Methods of reducing the bias by canceling the correlation components using the prediction error method [PEM adaptive feedback cancellation (AFC)] have been proposed[6], [7], [8]. However, it can be difficult to cancel the feedback signal using the PEM-AFC because the prediction filter eliminates the howling component[9], [10], [11] when the linear prediction filter converges more rapidly than the feedback path can be estimated.

In addition, feedback canceling algorithms[12], [13] based on the frequency domain binaural model (FDBM)[14] have been proposed. The method in those papers is straightforward and suppresses frequency bins that deviate from a database based on a binaural model according to the interaural level difference (ILD). These results indicate that the ILD calculated from the binaural signals can be used to detect howling, assuming that howling does not occur at the same frequency at the same time. However, it requires a high frequency resolution when it suppresses howling in a narrow band. Moreover, it may not be appropriate for hearing loss compensation because it limits the acoustic gain of the hearing aid.

In this paper, we first consider that it is possible to detect howling by using the ILD from binaural signals. Here we assume that if the sound source is far enough away from the head, it will not exceed the maximum value of the ILD at each frequency bin. Furthermore, for the convergence problem in PEM-AFC, we propose a binaural PEM-AFC that can control entrainment and howling by combining howling detect with an adaptive lattice filter using a correlation control algorithm[15]. The results of computer simulations to evaluate feedback estimation error, howling margin, and output signal distortion demonstrate the effectiveness of the proposed method.

This paper is organized as follows. Section II reviews the problems with using a feedback canceller for a closed-loop and the PEM-AFC algorithm. In Section III, we introduce the proposed method, the binaural PEM-AFC algorithm. The simulations presented in Section IV demonstrate the effectiveness of the proposed algorithm, and we conclude the paper in Section V.

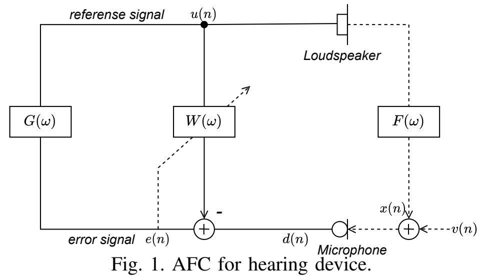

Fig. 1. AFC for hearing device.

II. Adaptive Feedback Cancellation

A. Adaptive feedback cancellation

In this section, we first describe a general feedback cancellation system for hearing aids. Figure 1 illustrates a general AFC system[1]. In this case, the closed-loop transfer function can be expressed as

$$C(\omega) = \frac{G(\omega)}{1 - G(\omega)[F(\omega) - W(\omega)]}, \tag{1}$$

where ω is a angular frequency for defining the transfer function. Here, $G(\omega)$ denotes the transfer function used for signal processing in the hearing aid, and $F(\omega)$ represents the transfer function from the loudspeaker to the microphone. The estimated feedback transfer function is denoted by $W(\omega)$. Therefore, the closed-loop can be canceled when $W(\omega)$ matches $F(\omega)$. In addition, $v(n)$ is the input signal to the system, and $x(n)$ is the feedback signal. The observed signal, which is denoted by $d(n)$, is the sum of $v(n)$ and $x(n)$, where n denotes a variable that represents the discrete time.

$$d(n) = v(n) + x(n), \tag{2}$$

$$x(n) = \boldsymbol{u}(u)\boldsymbol{f}(n)^T, \tag{3}$$

$$e(n) = d(n) - \hat{x}(n), \tag{4}$$

$$\hat{x}(n) = \boldsymbol{u}(u)\boldsymbol{w}(n)^T, \tag{5}$$

where

$$\boldsymbol{u}(n) = [u(n), u(n-1), ..., u(n-N+1)], \tag{6}$$

$$\boldsymbol{f}(n) = [f_1(n), f_2(n), ...f_L(n)], \tag{7}$$

The normalized LMS (NLMS[16]) update formula that is typically used for adaptive filters is given by

$$\boldsymbol{w}(n+1) = \boldsymbol{w}(n) + \mu \frac{e(n)\boldsymbol{u}(n)}{\boldsymbol{u}(n)\boldsymbol{u}(n)^T + \delta}, \tag{8}$$

where

$$\boldsymbol{w}(n) = [w_1(n), w_2(n), ...w_N(n)], \tag{9}$$

and δ is a very small constant to avoid dividing by zero.

B. Prediction-error-method-based adaptive feedback cancellation (PEM-AFC)

The estimation bias of the closed-loop is expressed[4] as

$$\text{bias}\{\boldsymbol{w}(n)\} = E\{\bar{\boldsymbol{R}}_u^{-1}\bar{\boldsymbol{p}}_{uv}\} = \boldsymbol{R}_u^{-1}\boldsymbol{p}_{uv}, \tag{10}$$

where,

$$\bar{\boldsymbol{p}}_{uv} = \frac{1}{n}\boldsymbol{U}\boldsymbol{v}, \tag{11}$$

$$\boldsymbol{U} = [\boldsymbol{u}(n)^T, \boldsymbol{u}(n-1)^T, ..., \boldsymbol{u}(1)^T], \tag{12}$$

$$\boldsymbol{v} = [v(n), v(n-1), ..., v(1)]^T. \tag{13}$$

Note that $\boldsymbol{R}_u$ is the $(N \times N)$ autocorrelation matrix of $\boldsymbol{u}(n)$, and $\boldsymbol{p}_{uv}$ is the $(N \times 1)$ cross-correlation vector between $\boldsymbol{u}(n)$ and $\boldsymbol{v}(n)$. Therefore, $\boldsymbol{u}(n)$ and $\boldsymbol{v}(n)$ must be orthogonal to obtain the optimal filter coefficients, which are denoted by $\boldsymbol{w_o}$.

However, the strong correlation between the reference signal and the incoming signal is unavoidable in low latency hearing devices. In consequence, the estimation error caused by the bias can distort the input signal and produce entrainment. The PEM-AFC has been proposed to solve this problem. This method assumes that the observed signal can be represented by the autoregressive (AR) model of the white noise. Figure 2 shows a block diagram of the PEM-AFC algorithm, where $\hat{A}(\omega)$ is the estimation of $A(\omega)$, and $A(\omega)$ transforms the desired signal with colored components into white noise $v_w(n)$.

The update formula is expressed as follows:

$$\boldsymbol{w}(n+1) = \boldsymbol{w}(n) + \mu \frac{e_p(n)\boldsymbol{u_p}(n)}{\boldsymbol{u_p}(n)\boldsymbol{u_p}(n)^T + \delta}, \tag{14}$$

where

$$\boldsymbol{u_p}(n) = [u_p(n), u_p(n-1), ...u_p(n-N+1)]. \tag{15}$$

Note that when howling occurs, the AR model decorrelates not only the observed signal $v(n)$ but also the howling component $x(n)$. Consequently, it may be difficult to suppress howling if the feedback path changes.

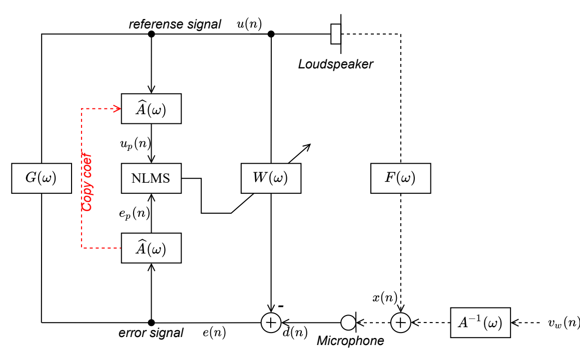

Fig. 2. Schematic illustration of PEM-AFC.

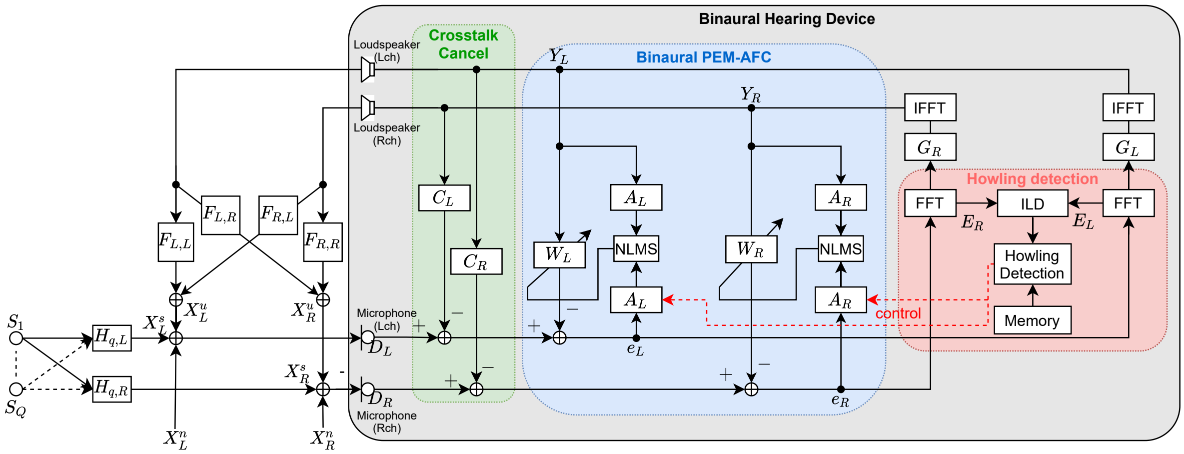

Fig. 3. Block diagram of proposed binaural feedback cancellation method.

III. Binaural PEM-AFC

A. Howling detection using head-related transfer functions

As described in the previous section, howling suppression may be degraded if the oscillation frequency component is removed by signal decorrelation, although it is effective for estimating the feedback path using an input signal with high autocorrelation. To solve this problem, it is necessary to discriminate between signals with high autocorrelation from outside the ear and howling signals between the loudspeaker and microphone of the hearing aid. However, it is extremely difficult to discriminate between these signals using a monaural signal.

In this section, we propose a binaural feedback canceller that can control the parameters of the decorrelation filter of the PEM-AFC. We assume that the binaural signals of channels mounted on the left and right ears can be obtained, and howling is identified using the ILDs of the input signals. Consequently, howling can be suppressed by preventing the decorrelation of the howling component, which is a problem in the conventional PEM-AFC, when howling is detected. Moreover, even if a sound source with high autocorrelation is input, it can be expected that the adaptive filter will be updated correctly and the feedback component will be removed.

Note that in this study, the proposed binaural algorithm was examined assuming that the crosstalk component from the loudspeaker of the hearing aid to the microphone is known and completely canceled. Figure 3 shows a block diagram of our proposed method. Uppercase and lowercase letters indicate the frequency domain and time domain, respectively.

In this figure, $H_{q,I}(\omega)$ $(I \in L, R)$ represents the transfer function from the qth $(q = 1, 2, ..., Q)$ sound source signal $S_q(\omega)$ to the left and right ears. $F_{L,L}(\omega)$ and $F_{R,R}(\omega)$ are the feedback transfer functions from the hearing aid loudspeaker to the microphones in the left and right ears, respectively, and $F_{L,R}(\omega)$ and $F_{R,L}(\omega)$ are the crosstalk transfer functions from the loudspeaker in the left and right ears to the microphone in the opposite ear. Furthermore, $Y_I(\omega)$ is the output signal from the hearing aid loudspeaker, $D_I(\omega)$ is the input signal to the hearing aid microphone, and $G_I(\omega)$ is the gain function of the left and right hearing aids.

In this block diagram, the green part represents crosstalk cancellation, the blue part represents the binaural PEM-AFC, and the red part represents howling detection. When howling is identified in the red part, howling is suppressed by controlling the linear prediction filter that decorrelates the signal. Each signal is defined as follows.

$$X_I^s(\omega) = \sum_{q=1}^{Q} S_q(\omega) H_{q,I}(\omega) \qquad I \in L, R, \tag{16}$$

$$X_I^u(\omega) = Y_L(\omega) F_{L,I}(\omega) + Y_R(\omega) F_{R,I}(\omega). \tag{17}$$

Here, $X_I^s(\omega)$ is the superimposed signal of each sound source observed by the left and right microphones, and $X_I^u(\omega)$ is the feedback signal from the hearing aid loudspeaker to the microphone. Therefore, the actual input signal vector to the microphone, $\mathbf{d}$, can be defined as follows.

$$\mathbf{d} = \mathbf{x^s} + \mathbf{x^u} + \mathbf{x^n} = \mathbf{sH} + \mathbf{yF} + \mathbf{x^n}, \tag{18}$$

where

$$\mathbf{d} = [D_L(\omega) \quad D_R(\omega)], \tag{19}$$

$$\mathbf{x^s} = [X_L^s(\omega) \quad X_R^s(\omega)], \tag{20}$$

$$\mathbf{x^u} = [X_L^u(\omega) \quad X_R^u(\omega)], \tag{21}$$

$$\mathbf{x^n} = [X_L^n(\omega) \quad X_R^n(\omega)], \tag{22}$$

and

$$\mathbf{s} = [S_1(\omega), S_2(\omega), ..., S_Q(\omega)], \tag{23}$$

$$\mathbf{y} = [Y_L(\omega) \quad Y_R(\omega)], \tag{24}$$

$$\mathbf{H} = \begin{pmatrix} H_{1,L}(\omega) & H_{1,R}(\omega) \\ H_{2,L}(\omega) & H_{2,R}(\omega) \\ \vdots & \vdots \\ H_{Q,L}(\omega) & H_{Q,R}(\omega) \end{pmatrix}, \tag{25}$$

$$\mathbf{F} = \begin{pmatrix} F_{L,L}(\omega) & F_{L,R}(\omega) \\ F_{R,L}(\omega) & F_{R,R}(\omega) \end{pmatrix}. \quad (26)$$

Note that $\mathbf{x^n}$ represents the background noise observed in the left and right ears.

When a sound source exists and a human hears the sound, there is generally a level difference between the ears depending on the position of the sound. Because this ILD does not depend on the sound source itself but on the sound source position, the maximum value of the ILD can be predicted using head-related transfer functions (HRTFs). In addition, assuming that howling does not occur in both ears at the same time and the same frequency in a hearing aid worn on both ears, the ILD at the time howling occurs is considered to be much larger than the level difference depending on the sound source position. Therefore, howling can be detected by constantly monitoring the ILD, and the PEM-AFC can be controlled. In the red part of Fig. 3, the estimated feedback and estimated crosstalk are subtracted from the binaural input signals of the hearing aid. The subtracted signal vector $\boldsymbol{e}_I(\eta)$ is transformed into the frequency domain by fast Fourier transform (FFT) analysis, and after smoothing, the ILDs are calculated.

$$\boldsymbol{e}_I(\eta) = [e_I(n), e_I(n-1), ..., e_I(n-L_f+1)], \quad (27)$$

$$\boldsymbol{E}_I(\eta, \omega_k) = \mathrm{FFT}[\boldsymbol{e}_I(\eta)], \quad (28)$$

$$\tilde{\boldsymbol{E}}_I(\eta, \omega_k) = \beta \tilde{\boldsymbol{E}}_I(\eta-1, \omega_k) + (1-\beta)|\boldsymbol{E}_I(\eta, \omega_k)|, \quad (29)$$

$$ILD(\eta, \omega_k) = 20 \log_{10} \left[\frac{\tilde{\boldsymbol{E}}_R(\eta, \omega_k)}{\tilde{\boldsymbol{E}}_L(\eta, \omega_k)} \right], \quad (30)$$

where η, L_f, and ω_k represent the frame number, frame length, and index number representing the frequency from the FFT, respectively.

Figure 4 shows the maximum absolute values of the ILDs in each frequency band obtained in advance using HRTFs [18]. Here, the horizontal and vertical axes show the frequency and maximum ILD [dB], respectively. ILDs generally vary depending on the sound source position. Our system uses $\psi(\omega_k)$, which is the maximum value of the ILDs, and the values are within a certain range depending on the frequency at which a directional source signal reaches the microphones of both ears. The $\psi(\omega_k)$ is stored in a memory to detect howling by comparison with the ILD of the input signal.

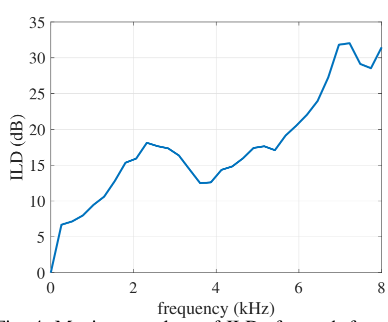

Fig. 4. Maximum values of ILDs for each frequency.

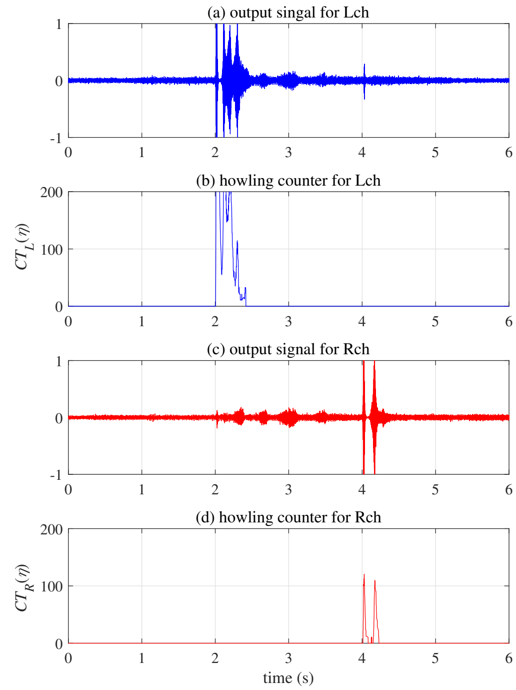

Fig. 5. Variation of howling counter with changes in feedback pass. The pass changes at 2 and 4 s for the left and right channels, respectively. A sound source is located at 0°.

$$CT_R(\eta) = \sum_{\omega_k} h_R(\eta, \omega_k) \cdot \{\, ILD(\eta, \omega_k) - \psi(\omega_k) \,\}, \quad (31)$$

where

$$h_R(\eta, \omega_k) = \begin{cases} 1 & (\quad ILD(\eta, \omega_k) - \psi(\omega_k) > 0 \quad) \\ 0 & (\quad \text{otherwise} \quad), \end{cases} \quad (32)$$

and

$$CT_L(\eta) = \sum_{\omega_k} h_L(\eta, \omega_k) \cdot \{\, |ILD(\eta, \omega_k)| - \psi(\omega_k) \,\}, \quad (33)$$

where

$$h_L(\eta, \omega_k) = \begin{cases} 1 & (\quad ILD(\eta, \omega_k) + \psi(\omega_k) < 0 \quad) \\ 0 & (\quad \text{otherwise} \quad). \end{cases} \quad (34)$$

When howling occurs and absolute value of the ILD exceeds $\psi(\omega_k)$, which is the maximum value of the ILD obtained in advance, $h_I(\eta, \omega_k) = 1$. Therefore, the value of the howling counter $CT_I(\eta)$ in Eq. (31) and (33) increases, and howling can be detected.

Figure 5 shows the change in the howling counter $CT_I(\eta)$ when howling is generated by changing the feedback path of the left channel at 2 s and that of the right channel at 4 s after the computer simulation begins. The figure shows (a) the left channel output waveform, (b) the left channel howling counter, (c) the right channel output waveform, and (d) the right channel howling counter. Figure 5(b) and (d) show that the value of $CT_I(\eta)$ changes when howling occurs, and howling can be detected. In this simulation, the sound source

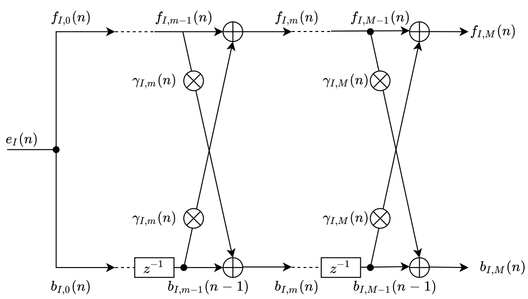

Fig. 6. Burg lattice algorithm.

position was set to 0°, which is in front of the hearing aid user, and traffic noise was also added. It was also confirmed that howling could be detected correctly even when the sound source position changed.

B. Howling cancellation using correlation control algorithm

The PEM-AFC algorithm decorrelates not only the external input signal but also the feedback signal, which may make howling control difficult. Here, we propose a binaural PEM-AFC algorithm that can control the howling signal by changing the decorrelation parameter in the PEM-AFC when howling is detected.

For the prediction error method [17], the Burg lattice algorithm (Eqs. 35–41) is used.

$$f_{I,0}(n) = d_I(n) - \boldsymbol{u}_I \boldsymbol{w}_I = d_I(n) - \hat{x}_I(n) = e_I(n), \quad (35)$$

$$b_{I,0}(n) = e_I(n), \quad (36)$$

$$\xi_{I,m}(n) = \lambda_{1,I}\xi_{I,m}(n-1) + (1-\lambda_{1,I})[f^2_{I,m-1}(n) + b^2_{I,m-1}(n-1)], \quad (37)$$

$$\kappa_{I,m}(n) = \lambda_2\kappa_{I,m}(n-1) + (1-\lambda_2)(-2)f_{I,m-1}(n)b_{I,m-1}(n-1), \quad (38)$$

$$\gamma_{I,m}(n) = \frac{\kappa_{I,m}(n)}{\xi_{I,m}(n)}, \quad (39)$$

$$f_{I,m}(n) = f_{I,m-1}(n) + \gamma_{I,m}(n)b_{I,m-1}(n-1), \quad (40)$$

$$b_{I,m}(n) = b_{I,m-1}(n-1) + \gamma_{I,m}(n)f_{I,m-1}(n). \quad (41)$$

It is known that when the lattice filter has a sufficient number of stages for signal decorrelation, the output signal does not contain the correlation component. We devised a PEM-AFC method to control the decorrelation effect using the correlation control algorithm proposed by Kawamura et al.[15]. Howling oscillation can be suppressed by applying the NLMS algorithm to a signal, which leaves a weak correlation component when howling is detected. The forgetting coefficient that is used to calculate the reflection coefficient of the lattice filter to control the effect of decorrelation is controlled. When the forgetting coefficient is set to $0 < \lambda_1 < \lambda_2 < 1$, the expected value of the reflection coefficient can be expressed by the following equation.

$$\lim_{n\to\infty} E[\gamma_m(n)] \approx \frac{E[\kappa_{m-1}(n)]}{E[\xi_{m-1}(n-1)]} = \alpha\frac{E[(-2)f_{I,m-1}(n)b_{I,m-1}(n-1)]}{E[f^2_{I,m-1}(n) + b^2_{I,m-1}(n-1)]}, \quad (42)$$

where

$$\alpha = (1-\lambda_2)/(1-\lambda_1). \quad (43)$$

Here, when $\alpha = 1$, which implies $\lambda_1 = \lambda_2$, the equation is equivalent to that of a general adaptive lattice filter, and the autocorrelation component is removed. On the other hand, when $\alpha = 0$, that is $\lambda_2 = 1$, the autocorrelation component is completely preserved. That is, autocorrelation components can be controlled by setting λ_1 and λ_2. By exploiting these properties, when the howling counter judgment exceeds a predetermined threshold value, the forgetting coefficient is set as follows, and correlation control is performed.

$$\lambda_{1,I} = \begin{cases} \tilde{\lambda} & (CT_I(\eta) > T_C) \\ \lambda_2 & (\text{otherwise}). \end{cases} \quad (44)$$

IV. Experiments

A. Experimental conditions

An experiment was conducted using a computer simulation to evaluate the effectiveness of the proposed method. The following items were evaluated.

1) *Misalignment (MIS)*
2) *Maximum stable gain (MSG)*
3) *Spectral distortion level (SDL)*

The algorithms to be evaluated for comparison are the NLMS algorithm (AL1), the PEM-AFC (AL2), and the proposed method (AL3). Table 1 shows the parameters used in the evaluation experiments. A male voice from the IEEE voice corpus[19] was used as the first sound source. As the second source, an automobile back-up beeper was used as a periodic signal that induces entrainment. For background noise, we used traffic noise recorded binaurally using a dummy head

TABLE I
Parameters used in evaluation experiments

sampling frequency	16000 Hz
frame length L_f	64
adaptation algorithm (AFC)	NLMS
adaptive filter tap N	64
step size μ	0.01
linear prediction error method	Burg lattice
number of lattice stages M	32
forgetting factor for lattice filter $\tilde{\lambda}$	0.99
forgetting factor for lattice filter λ_2	0.999
forgetting factor β	0.95
threshold Tc	5
normalization constant δ	$6e^{-7}$

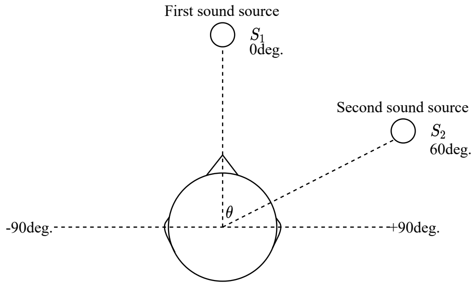

Fig. 7. Relative locations of hearing aid user, sound source 1, and sound source 2 in experimental computer simulation.

(KEMAR, GRAS) placed on the side of a congested road. The first and second sources were convolved with HRTFs to add directional information.

First, impulse responses (96 tap) were used for the feedback and crosstalk transfer functions of the left and right ears in the hearing aid simulation, which were measured with the dummy head wearing an BTE (behind the ear) hearing aid with open-type eartip. However, to induce howling, the feedback gain was intentionally changed by 6 dB at 16 and 20 s for the left ear and 14 and 17 s for the right ear.

Figure 7 shows the relative positions of the sound source and hearing aid user. The first sound source was convolved by a 0° HRTF so that it was located in front of the hearing aid user. Next, the position of the second sound source, θ, was changed in 10° increments from $-90°$ on the left-hand side to $+90°$ on the right-hand side to confirm the robustness of howling detection relative to the correlated sound source location. Note that the true impulse response is used for the crosstalk cancellation part because it is assumed that the crosstalk transfer function is known and does not vary.

B. Evaluation results

Examples of the output waveform and spectrogram are shown in Figs. 8 and 9, respectively, when S_1 is located at 0° and S_2 is located at $+60°$. Note that Fig. 9 shows only the back-up beeper sound section (7 to 13 s) of the output signal for each algorithm. Figure 8 shows (a) the reference output waveform and the output waveforms of (b) AL1, (c) AL2, and (d) AL3. The input signals include background noise, speech signals (4 to 7 s), the back-up beeper (7 to 13 s), and howling signals (14 to 20 s). Note that the reference signal is the output signal after ideal processing without feedback and crosstalk; therefore, it does not contain howling and entrainment.

As shown in Fig. 8, the output waveform of AL1 converged more rapidly than that of AL2 when howling occurred. The output waveform of AL3 converged as rapidly as that of AL1 when howling occurred. Next, as shown in Fig. 9, the spectrogram of AL1 showed signal distortion in the back-up beeper section because AL1 distorts the strongly autocorrelated input signal. By contrast, the spectrograms of AL2 and AL3 showed output similar to the reference signal, and the distortion of the output signal in the back-up beeper section was quite small.

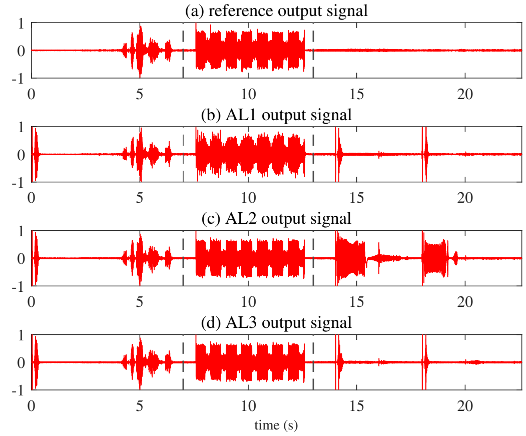

Fig. 8. Output waveform of each algorithm.

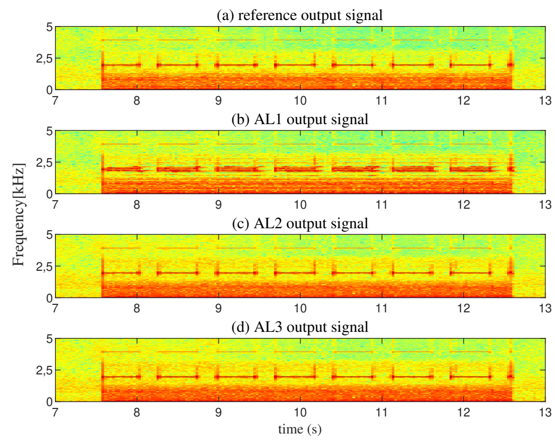

Fig. 9. Spectrogram of output signal of each algorithm. Note that these spectrograms were calculated using only the part of the output signal from 7 to 13 s, which is an automobile back-up beeper.

These results demonstrate that AL3 suppresses howling and entrainment effectively, and it has the advantages over both AL1 and AL2.

1) Misalignment (MIS): The MIS is evaluated to confirm the error of the feedback $W_I(\omega_k)$ estimated by the NLMS method to estimate the feedback transfer function

$$MIS_I(\eta,\theta) = 20\log_{10}\left[\frac{\|\boldsymbol{f}_{I,I}(\eta)-\boldsymbol{w}_I(\eta)\|_2}{\|\boldsymbol{f}_{I,I}(\eta)\|_2}\right], \qquad (45)$$

where $\boldsymbol{f}_{I,I}(\eta)$ represents the impulse response vector of the feedback transfer functions $F_{I,I}(\omega_k)$, and $\boldsymbol{w}_I(\eta)$ is the impulse response vector of the estimated value $W_I(\omega_k)$ of the feedback transfer function, which varies with θ and η. The evaluation value is calculated as the long-term average of Eq. (45).

Figure 10(a) and (b) show the results of the MIS evaluation experiments in the left and right channels, respectively. The horizontal and vertical axes show the arrival direction of the

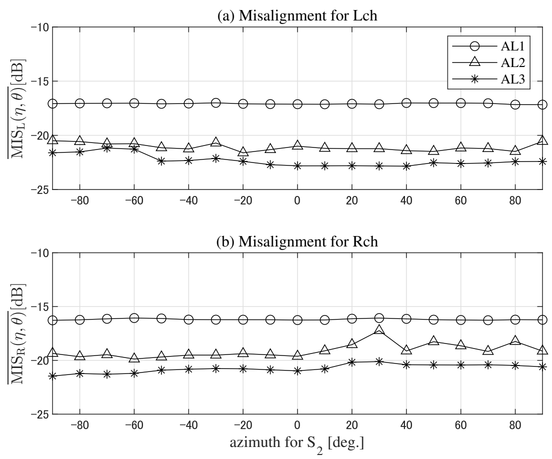

Fig. 10. MIS score for each algorithm when the arrival direction of the second sound source changes.

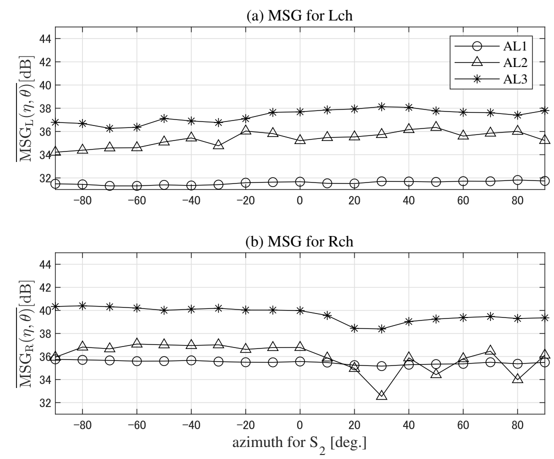

Fig. 11. MSG score of each algorithm when the arrival direction of the second sound source changes.

second sound source S_2 [deg] and the long-term average value of $\overline{MIS_I(\eta, \theta)}$ [dB].

In both Fig. 10(a) and (b), the evaluation value of AL1 was larger than those of AL2 and AL3. The reason is that the presence or absence of a decorrelation filter in the periodic signal component of the second source caused errors in feedback estimation by the NLMS algorithm, resulting in entrainment. Although the difference between the values of AL2 and AL3 was small, AL3 scored better in terms of faster feedback suppression. The reason for the small difference is thought to be that the feedback time is only a few seconds, and the evaluation values are averaged, making it difficult to see a difference.

2) Maximum stable gain (MSG): The MSG evaluation confirmed the effectiveness of the hearing aid's feedback suppression algorithm. It was calculated from the largest obtainable stable gain (howling margin). The following formula was used for this evaluation.

$$ASG_I(\eta, \omega_k, \theta) = \frac{F_I(\eta, \omega_k)}{\{F_I(\eta, \omega_k) - W_I(\eta, \omega_k, \theta)\} G_I(\eta, \omega_k)} \tag{46}$$

$$MSG_I(\eta, \theta) = \max_{\omega_k} \{20 \log_{10} |ASG_I(\eta, \omega_k, \theta)|\}. \tag{47}$$

Eq. (47) calculates the margin to howling (added stable gain, ASG) for each frequency. By contrast, the MSG is obtained from the ASG at the frequency with the lowest margin to howling.

Figure 11(a) and (b) show the long-term average of the MSG, $\overline{MSG_I(\eta, \theta)}$, for each channel. The horizontal and vertical axes show the arrival direction angle of the second sound source S_2 and the MSG, respectively. The MSG of AL3 was higher than those of AL1 and AL2. Because the MSG used the minimum margin to howling among all the frequencies, there are large differences between AL1, AL2, and AL3. Therefore, AL3 can apply a higher gain without howling compared to AL1 and AL2.

3) Spectral distortion level (SDL): The sound quality of the output signal from the loudspeaker was evaluated using the SDL. It was calculated from the spectral difference of the output and references signals, and it quantified the degree of sound quality degradation caused by entrainment and howling. The SDL is defined as

$$SDL_I(\theta) = 10 \log_{10} \frac{\sum_{\eta} \sum_{\omega_k} \{|Y_I^{\mathrm{ref}}(\eta, \omega_k, \theta)| - |Y_I(\eta, \omega_k, \theta)|\}^2}{\sum_{\eta} \sum_{\omega_k} |Y_I^{\mathrm{ref}}(\eta, \omega_k, \theta)|^2}, \tag{48}$$

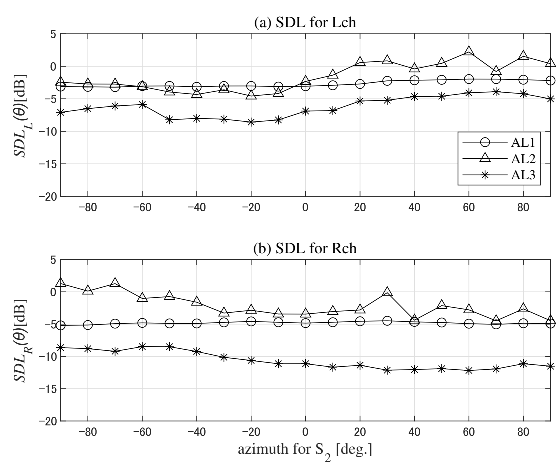

Fig. 12. SDL score of each algorithm when the arrival direction of the second sound source changes.

where Y_I^{ref} is the reference signal, and Y_I is the output signal of each algorithm. Figure 12(a) and (b) show the results of SDL evaluation experiments for each algorithm in the left and right channels. The horizontal and vertical axes show the angle of the arrival direction of the second sound source S_2 and the SDL evaluation value $SDL_I(\theta)$, respectively.

The results show that the SDL of AL1 was increased by entrainment, and that of AL2 was increased by howling. By contrast, AL3 can suppress both entrainment and howling, and the SDL of AL3 was significantly lower than those of AL1 and AL2.

V. Conclusion

We proposed a binaural PEM-AFC algorithm that extends the PEM-AFC to binaural hearing devices and solves the problem of howling control caused by decorrelated feedback signals. In developing the proposed method, we focused on the fact that the occurrence of howling can be detected from the ILD between the right and left ears calculated from binaural signals. By combining the correlation control algorithm for an adaptive lattice filter with the PEM-AFC, we showed that the algorithm could achieve rapid convergence under conditions where it is difficult to suppress howling using conventional PEM methods. In addition, simulation experiments showed that the proposed method could robustly discriminate between the input and feedback signals even when the angle of incidence of the autocorrelated input signal changed. Evaluation tests that examined the MIS, MSG, and SDL demonstrated the superiority of the proposed method over the conventional bilateral algorithm in which left and right devices operate independently.

References

[1] J. M. Kates,"Digital Hearing Aids," *Plural Publishing, San Diego,* 2008.

[2] T. van Waterschoot and M. Moonen, "Fifty years of acoustic feedback control: State of the art and future challenges," *Proc. IEEE,* vol. 99, no. 2, pp. 288–327, Feb. 2011.

[3] J. Hellgren and U. Forssell, "Bias of feedback cancellation algorithm in hearing aids based on direct closed-loop identification," *IEEE Trans. Speech Audio Process.* vol. 9, no. 7, pp. 906–913, Nov. 2001.

[4] B. C. Bispo, C. F. Yamamura, W. M. S.'Nogueira, E. A. Theodoro, and P. M. Rodrigues, "Analysis of acoustic feedback cancellation system based on direct closed-loop identification," *J. Commun. Inf. Syst.* vol. 35, no. 1, pp. 217–229, 2020.

[5] M. T. Akhtar and A. Nishihara, "Howling and entrainment in hearing aids: A review," *Eng. J.* vol. 20, no. 5, pp. 5–13, 2016.

[6] A. Spriet, I. Proudler, M. Moonen, and J. Wouters, "Adaptive feedback cancellation in hearing aids with linear prediction of the desired signal," *IEEE Trans. Sig. Process.* vol. 55, no. 10, pp. 3749–3763, Oct. 2005.

[7] T. van Waterschoot, G. Rombouts, and M. Moonen, "On the performance of decorrelation by prefiltering for adaptive feedback cancellation in public address system," *in Proceedings of 4th IEEE Benelux Signal Processing Symposium, Hilvarenbeek, The Netherlands*, pp. 167–170, April 2004.

[8] G. Bernardi, T. van Waterschoot, J. Wouters, and M. Moonen, "Adaptive feedback cancellation using a partitioned-block frequency-domain Kalman filter approach with PEM-based signal prewhitening," *IEEE Trans. Audio Speech Lang. Process.* vol. 25, no. 9, pp. 1784–1798, Sep. 2017.

[9] K. Kashima, A. Kawamrura, M. Sunohara, K. Nishiyama, N. Hiruma, and Y. Iiguni, "Adaptive feedback canceller with howling detection for hearing aids," *in Proceedings of the APSIPA Annual Summit and Conference*, pp. 704–710, 2015.

[10] N. Hiruma, C. Haruta, M. Sunohara, M. Tateno, and K. Nishiyama, "Whiten Fast H_∞ filter based on prediction error method for adaptive feedback cancellation in hearing aids," *Signal Processing Symposium*, pp. 326–331, in Japanese. Nov. 2017.

[11] S. Nordholm, H. Schepker, L.T.T. Tran, and S. Doclo, "Stability-controlled hybrid adaptive feedback cancellation scheme for hearing aids," *J. Acoust. Soc. Am.*, vol. 143 no.1, pp. 150–166, Jan. 2018.

[12] T. Udagawa, K. Matsuo, S. Kawano, H. Nakashima, and Y. Chisaki, "A simple howling control for binaural hearing aid system," *ICSV12*, 2005.

[13] Y. Chisaki, K. Matsuo, and T. Udagawa, "Howling canceler using interaural level difference for binaural hearing assistant system," *Acoust. Sci. Tech.* vol. 28, no. 2, pp. 90–97, 2007.

[14] H. Nakashima, Y. Chisaki, T. Usagawa, and M. Ebata, "Frequency domain binaural model based on interaural phase and level differences," *Acoust. Sci. Tech.* vol. 24, no. 4, pp. 172–178, 2003.

[15] A. Kawamura and Y. Iiguni, "A colored noise suppressor using lattice filter with correlation controlled algorithm," *Audio Engineering Society 125th Convention*, Oct. 2–5, 2008.

[16] S. Haykin, "Adaptive Filter Theory," *3rd ed.*, 1991.

[17] S. Haykin, "Introduction to Adaptive Filters," *Macmillan Publishing Company, New York*, 1984.

[18] B. Gardner and K. Martin, "HRTF measurements of a KEMAR dummy-head microphone," http://sound.media.mit.edu/resources/KEMAR.html

[19] "297-1969 - IEEE Recommended Practice for Speech Quality Measurements," *IEEE*, https://ieeexplore.ieee.org/document/7405210